

Adapting Neural Models with Sequential Monte Carlo Dropout

Pamela Carreno-Medrano Dana Kulić Michael Burke

Department of Electrical and Computer Systems Engineering
Monash University
Australia

{pamela.carreno, dana.kulic, michael.g.burke}@monash.edu

Abstract: The ability to adapt to changing environments and settings is essential for robots acting in dynamic and unstructured environments or working alongside humans with varied abilities or preferences. This work introduces an extremely simple and effective approach to adapting neural models in response to changing settings. We first train a standard network using dropout, which is analogous to learning an ensemble of predictive models or distribution over predictions. At run-time, we use a particle filter to maintain a distribution over dropout masks to adapt the neural model to changing settings in an online manner. Experimental results show improved performance in control problems requiring both online and look-ahead prediction, and showcase the interpretability of the inferred masks in a human behaviour modelling task for drone tele-operation.

Keywords: Model Adaptation, Online Robot Control and Prediction

1 Introduction

Neural models and policies are now ubiquitous in modern robotics. The prevailing approach to training these follows a two stage process – a large, comprehensive collection of data (often state and action pairs) is used to train a suitable model or policy, which is then frozen and deployed. Unfortunately, this results in models that are unable to adapt to changes in the environment, which is a particular concern in robotics. For example, it would be preferable for a robot dynamics model to handle context dependent kinematic or dynamic properties, or a collaborative robot relying on predictions of human behaviour to adapt to different human abilities or preferences. Many existing adaptive control techniques [1] attempting to tackle this problem rely on carefully considered parametric models, but these may lack the requisite capacity for prediction that is typically associated with neural models. In contrast, meta-learning and adaptive neural control approaches addressing this problem are often quite cumbersome to train and implement.

This paper introduces a simple and effective approach to achieve adaptation for neural network models. First we train a model, $f_{\theta}(\cdot)$ using dropout [2], on data gathered from different settings or tasks. Dropout can be considered analogous to randomly masking neurons in the network, producing an ensemble of predictive models, or a distribution over possible outputs [3]. At run-time, a particle filter is used to update the dropout mask, depending on the predictive quality of the model, so as to condition the network to operate in a given context. This allows for neural models that can easily and rapidly adapt to changes in the environment or behaviour of a human collaborator in online settings.

Results show that this simple-to-implement approach improves upon a more complex first-order meta-learning training strategy, and can alleviate potential failures due to catastrophic forgetting. Moreover, we show that the resulting masks can be interrogated to obtain additional information about the adaptations required for particular contexts. We also show how this information can be leveraged in a human modelling application to answer questions about a given user. In summary, the core contributions of this work are to show that: (1) sequential Monte Carlo dropout is an effective technique for online model adaptation and control in rapidly changing settings, and (2) the masks

inferred by this process provide a context-dependent ‘signature’ that is of particular value for human behaviour modelling in support of personalised robot decision making.

2 Background and Related Work

Model adaptation: Model adaptation in an online fashion is a core focus of adaptive control [1], and typically involves the design of a suitable observer or estimation scheme [4] to infer parameters of interest. Many of these system identification approaches [5, 6, 7, 8, 9] rely on models conditioned on known physical properties like friction, mass and gravity, and infer these from data. These approaches require knowledge of the parametric form of uncertainty and are only feasible for very specific model structures [10]. Our approach introduces an adaptation mechanism applicable to more general predictive neural models.

For deep learning, model adaptation can be studied as a generalisation problem in a meta-learning context. Popular approaches like model agnostic meta-learning (MaML) [11] seek to learn network weights that can be easily adapted for different tasks by gradient descent via specialised training regimes that alternate between task specific training and maintaining a representation that is well suited to multiple tasks. Although time-consuming, faster, first-order meta-learning approximations such as Reptile [12] have proven relatively effective. The idea of enhancing generalisation by learning well-structured internal representations underpins a number of works such as ProtoNet [13] and Relation networks [14], alongside more recent approaches that rely on multi-task training with an explicit learned auxiliary input [15, 16] that can be adapted online. Our approach can also be viewed through a representation learning lens, in that masks ‘prime’ the network to produce context dependent outputs. This representation-priming perspective also aligns with recently developed transformer-based architectures tackling meta-learning (e.g., [17, 18, 19]). Here, key embeddings are used to unlock network components required for context specific prediction. The dropout mask used in our work is analogous to a transformer key that is inferred at run time.

Several works targeting online model adaptation have argued that we should ideally update our models and beliefs in response to evidence in a Bayesian fashion. This approach is taken in elastic weight consolidation, which aims to reduce the plasticity of network weights that are important to a task [20]. There is also some evidence that MaML can be reinterpreted as a Bayesian hierarchical model [21, 22]. Dropout [2] is a popular regularisation technique for neural network training, and has also been used to represent prediction uncertainty in deep learning [3]. We leverage dropout within a sequential importance sampling framework to provide an explicit Bayesian update rule for mask inference and model adaptation. Like [20], this preserves connections important to a task.

As an alternative to back-propagation, evolutionary, sampling-based approaches to training neural models [23, 24, 25] have been explored and shown to be effective in a reinforcement learning context [26]. Similarly, the cross entropy method is a popular technique for global sampling-based optimisation and planning [27, 28]. Pathnet [29] uses evolution to find the neural network pathways that should be trained for specific tasks. Particle filtering has also been used to prune neural networks for compression [30]. Our work is similar, but considers the online adaptation case and samples dropout masks to infer a distribution over masks, rather than considering all weights and connections.

Human modelling: The dropout mask inferred at run-time using our approach can be considered as an embedding or summary of the context-specific adaptation required by the network at a given time step. This is valuable for adaptive human modelling in shared-autonomy and similar collaborative applications, where context-specific masks could help guide the type of assistance offered to an operator. Human behaviour models help robots to understand human preferences, predict future human actions, and adapt to changes in human behaviour. Two general approaches to human behaviour modelling are the most common in robotic applications. The first postulates that humans are rational agents whose actions are in accordance with some (un)known intentions and rewards [31]. To account for human variability and diversity in behaviour – in particular deviations from optimal action choices, these models are augmented with computational interpretations of high-level decision factors such as trust [32], expertise [33], fatigue [34], and adaptability [35], among others. These factors can be inferred in an online manner during interaction, thus allowing robots to adapt their responses to different human users (e.g., [36]). Often preferred because of their simplicity and interpretability, these models suffer two main drawbacks. First, they strongly rely on simplistic parametric model structures, which can limit model expressivity and predictive power. In particular,

most models assume that a single high-level decision factor is sufficient to capture and explain most of the observed human behaviour (e.g., [36]). Second, to make inference tractable in real-time, these approaches are often limited to simplified state and action space representations, and further assume that the model parameters remain stationary for the duration of the whole interaction (e.g., [35]). Our approach aims to relax these constraints by introducing an adaptation mechanism that can be used with more general predictive and expressive neural models and that also captures changing behaviour.

In the second family of approaches, collected human behaviour data is used to train machine learning models that predict future behaviour (i.e., imitation learning) [37, 38, 39]. Because of their data-driven nature and assuming good quality data is provided during training, these models can implicitly capture most of the sources of variability in the observed human behaviour without making explicit assumptions about what those sources are. Thus, these models of human behaviour are no longer limited to single decision factors. However, this increase in model expressivity and predictive power comes at the cost of limited interpretability [40]. Furthermore, these models can fail to generalize and adapt to humans whose behaviour significantly differ from the training data set [16]. Our approach addresses the interpretability and adaptation limitations of imitation-based human models through the online estimation of dropout masks. As shown in Sec. 5, this mask inference process allows for successful local adaptation in extrapolation (to human users never seen during training). Similarly, we show that contextual information pertaining to high-level factors such as a human operator’s skill level and preferences can be queried through a simple k-nearest mask approach.

3 Method

We consider a standard Markov decision process, with \mathbf{x}_t denoting a state at time t , and R_t denoting the reward received at time t after transitioning from state \mathbf{x}_{t-1} to state \mathbf{x}_t , due to control action \mathbf{u}_t . Let $f_\theta(\cdot)$ be a neural network with parameters θ . Networks such as these are frequently trained to approximate dynamics models for future state prediction $\mathbf{x}_t \sim f_\theta(\mathbf{x}_{t-1}, \mathbf{u}_t)$, for reward prediction $R_t \sim g_\theta(\mathbf{x}_{t-1}, \mathbf{u}_t)$, or as policies for selecting an action given a state $\mathbf{u}_t \sim \pi_\theta(\mathbf{x}_t)$.

Our goal is to find a way of adapting a pre-trained network to changing settings in response to some deviation between predicted states, actions or rewards and those actually observed. Let $f_\theta(\cdot|\mathbf{M}_t)$ denote a neural network trained using dropout regularisation. Here \mathbf{M}_t represents a binary mask which suppresses or drops neurons in the network. When training with dropout, neurons are randomly masked during the forward pass. We do not consider any specialised training regime, and simply use multi-task training - samples drawn at random from a large training dataset.

We now show how this can be exploited to enable online adaptation. For convenience, we restrict the discussion below to a dynamics model setting where a neural network is trained to predict a state \mathbf{x}_t , given a previous state \mathbf{x}_{t-1} and action \mathbf{u}_t . However, it should be noted that the proposed approach can be used to adapt policies, reward predictors and in many other settings.

3.1 Online Mask Adaptation

We use the deviation between predicted \mathbf{x}_t and actual observations \mathbf{z}_t to form a Gaussian likelihood,

$$p(\mathbf{z}_t|\mathbf{M}_t) = \mathcal{N}(\mathbf{z}_t|f_\theta(\mathbf{x}_{t-1}, \mathbf{u}_t|\mathbf{M}_t), \Sigma), \quad (1)$$

where Σ denotes measurement noise. This likelihood measures the chances of making an observation given a dropout mask \mathbf{M}_t . Taking an ensemble view of model training with dropout, we aim to find the mask, and corresponding model, that results in the most accurate prediction in a given setting. Formally, our goal is to determine a posterior distribution over dropout masks $p(\mathbf{M}_t|\mathbf{z}_{1:t})$ conditioned on a series of observations $\mathbf{z}_{1:t}$. To do so, we formulate a sequential update rule

$$p(\mathbf{M}_t|\mathbf{z}_{1:t}) \propto p(\mathbf{z}_t|\mathbf{M}_t)p(\mathbf{M}_t|\mathbf{z}_{1:t-1}), \text{ where} \quad (2)$$

$$p(\mathbf{M}_t|\mathbf{z}_{1:t-1}) = \int p(\mathbf{M}_t|\mathbf{M}_{t-1})p(\mathbf{M}_{t-1}|\mathbf{z}_{1:t-1})d\mathbf{M}_{t-1}, \quad (3)$$

using an appropriate transition model $p(\mathbf{M}_t|\mathbf{M}_{t-1})$ for the dropout mask. In this work, we propose to randomly bit-flip some small fraction ($d\%$) of the mask for the transition model, $p(\mathbf{M}_t|\mathbf{M}_{t-1})$. This allows for some exploration over potential new masks and adaptation to new settings while

keeping existing masks close to those associated with networks best suited to current settings. Importantly, bit flipping can be efficiently computed using an xor operation.

Since the integral in (3) is intractable, we approximate it using importance sampling and hence reduce the computation of the posterior over masks to a bootstrap particle filter [41]. That is, we approximate the distribution over masks using a set of N weighted particles, $p(\mathbf{M}_t|\mathbf{z}_{1:t}) \approx \sum_{i=1}^N w_i \delta(\mathbf{M}_t^i)$, with weights $w_i \propto p(\mathbf{z}_t|\mathbf{M}_t^i)$, particle \mathbf{M}_t^i drawn from the transition distribution $p(\mathbf{M}_t^i|\mathbf{M}_{t-1}^i)$, and Dirac measure $\delta(\cdot)$ at point (\cdot) . A resampling step is used after each iteration to prevent particle degeneracy. This produces a distribution over masks and a corresponding posterior over the predicted state

$$p(\mathbf{M}_t|\mathbf{z}_{1:t}) \approx \frac{1}{N} \sum_{i=1}^N \delta(\mathbf{M}_t^i); \quad (4)$$

$$\begin{aligned} p(\mathbf{x}_t|\mathbf{x}_{t-1}, \mathbf{u}_t, \mathbf{z}_{1:t}) &= \int p(\mathbf{x}_t|\mathbf{x}_{t-1}, \mathbf{u}_t, \mathbf{z}_{1:t}, \mathbf{M}_t) p(\mathbf{M}_t|\mathbf{z}_{1:t}) d\mathbf{M}_t \\ &\approx \frac{1}{N} \sum_{i=1}^N \delta(f_\theta(\mathbf{x}_{t-1}, \mathbf{u}_t, \mathbf{M}_t^i)). \end{aligned} \quad (5)$$

For downstream tasks like control, where we are only interested in the adapted prediction model, we compute a minimum-mean squared error mask estimator

$$\bar{\mathbf{M}}_t = \frac{1}{N} \sum_{i=1}^N \mathbf{M}_t^i, \quad (6)$$

from the mask particles and use this to condition the network $f_\theta(\cdot)$. We note that since the likelihoods are bounded and we use a standard resampling scheme, convergence of the proposed approach is independent of the state dimension, with the rate of convergence in $\frac{1}{N}$ [42]. The filter also allows for variable particle sizes, which can be increased or decreased online depending on the effective particle size as defined by $N_{eff} = \frac{1}{\sum_{i=1}^N (w_i)^2}$ [43]. Algorithm 1 illustrates the adaptation process, which we term sequential Monte Carlo dropout (SMCD). We first sample N possible masks from the prior mask distribution by bit flipping, and then make a batch prediction of possible states for each mask. We then compute the likelihood for each mask using (1), normalise and re-sample, to obtain an approximate distribution over masks that gives predictions close to the observation. Finally, we compute a minimum-mean squared error mask, which can be used to condition the network in downstream tasks. The process repeats recursively and online.

A key benefit of this approach is that it does not change the underlying models learned. The original prediction can be recovered at any time, by simply restoring or resampling the mask. This is in contrast to approaches that continue to train or take gradient steps in response to errors, which may be suitable for continual learning, but are vulnerable to catastrophic forgetting [44, 20].

4 Experiments

We investigate model adaptation using SMCD both in simulation and with real-world human data. In simulation, we use a two-link arm with changing link lengths and a 7 Degree of Freedom (DOF)

Algorithm 1 Sequential Monte Carlo Dropout (SMCD) Model Adaptation

Input: Trained net f_θ , Observation sequence $\mathbf{z}_{1:T}$, Transition probability d , Measurement uncertainty Σ
Output: Mask estimate sequence $\bar{\mathbf{M}}_{1:T}$
 Initialise N random masks $\{\mathbf{M}_0^i\}_{i=1\dots N}$
for $t = 1 \dots T$ **do**
 for $i = 0 \dots N$ **do**
 Sample $\mathbf{M}_t^i \sim p(\mathbf{M}_t^i|\mathbf{M}_{t-1}^i)$ by bit-flipping
 Sample $\mathbf{x}_t^i = f_\theta(\mathbf{x}_{t-1}, \mathbf{u}_t|\mathbf{M}_t^i)$
 Evaluate $w^i = \mathcal{N}(\mathbf{z}_t|\mathbf{x}_t^i, \Sigma)$
 end for
 Draw N masks: $\{\mathbf{M}_t^i\}_{i=1\dots N} \sim \frac{\sum_{i=1}^N w_i \delta(\mathbf{M}_t^i)}{\sum_{i=1}^N w_i}$
 Compute best mask estimate $\bar{\mathbf{M}}_t = \frac{1}{N} \sum_{i=1}^N \mathbf{M}_t^i$
end for

Panda arm reaching task with varying end-effector length. We evaluate the performance of the proposed method in prediction and control using the two-link arm task and 7-DOF Panda reaching task respectively. The real-world data corresponds to a drone tele-operation scenario where operators of varying skill levels completed several landing tasks. This scenario illustrates mask interpretability by showing how different high-level characteristics (an operator’s landing strategy and skill level) can be determined by a simple mask comparison process. We refer the reader to the [Appendix](#) for additional experiments including applications to Reinforcement Learning (RL) settings.

4.1 Two-Link Arm Task (Forward Kinematics)

The 2-link arm follows the dynamics and forward kinematics:

$$\dot{q}_1 = u_1, \dot{q}_2 = u_2 \tag{7}$$

$$x = l_1 \cos(q_1) + l_2 \cos(q_1 + q_2), y = l_1 \sin(q_1) + l_2 \sin(q_1 + q_2). \tag{8}$$

We train neural models $f_\theta(\mathbf{q})$ to perform forward kinematics (predicting end-effector position $\mathbf{x} = [x, y]^T$ given joint angles $\mathbf{q} = [q_1, q_2]^T$) for variable limb lengths l_1, l_2 . Training data is gathered by randomly initialising $q_i \sim U(-\pi, \pi)$, and episodically motor babbling $u_i \sim \mathcal{N}(0, 1)$ for 10 steps. We generate 150 episodes for 1000 tasks, with fixed link lengths $l_i \sim \mathcal{N}(1, 0.3)$ in each task.

The two-link forward kinematics task is used to investigate the adaptation properties of SMCD in N -step look-ahead prediction after T adaptation steps¹. Specifically, we evaluate prediction error for an unknown manipulator with link lengths ($l_i \sim \mathcal{N}(1, 0.3)$) fixed over a motor babbling episode ($u_i \sim \mathcal{N}(0, 1)$), starting from a randomly sampled angle $q_i \sim U(-\pi, \pi)$. This evaluates the “interpolation” ability and suitability for receding-horizon model predictive control tasks. We benchmark against an oracle model, no adaptation, a latent variable model, and a model trained using Reptile [12], a first order meta-learning approach, and investigate adaptation using both gradient descent and SMCD.

4.2 7-DOF Panda Arm Reaching Task (Manipulator Control)

The 7-DOF Panda manipulator is simulated using the python robotics toolbox [45] with a tool that introduces an arbitrary unknown end-effector extension ($l \sim U(-0.5, 0.5)$). As with the two-link arm task, we train neural models $f_\theta(\mathbf{q})$ to perform forward kinematics (predicting end-effector position $\mathbf{x} = [x, y, z]^T$ given joint angles $\mathbf{q} = [q_1, \dots, q_7]^T$). Our goal is to drive the Panda from a fixed reference pose to within 5 cm of a randomly selected and kinematically feasible end-effector goal \mathbf{x}_g in less than 200 time steps. To reach the goal, we use the proportional-derivative (PD) control law $\mathbf{u} = -K_1 \mathbf{J}^\dagger (\mathbf{x} - \mathbf{x}_g) - K_2 \dot{\mathbf{q}}$, where \mathbf{J}^\dagger corresponds to the Jacobian of the end-effector position (\mathbb{R}^3) joint with respect to the angles (\mathbb{R}^7). We consider the case where measurement of the true end effector position is only available every n -th timestep, which requires model-reference control when measurements are not available. This measures the ability of the adapted model to generalise to global context changes under a realistic control setting in which observations are captured at a lower rate than the required controller frequency.

4.3 Drone Landing Task (Mask Interpretability)

We use the human data previously introduced in [46] for this task². This dataset comprises 528 tele-operation trajectories collected for 33 human operators (16 trajectories per operator) with different skill levels in a simulated environment. Here, operators were asked to pilot and land a drone on one of five platforms by providing linear velocity commands through keyboard inputs. As shown in Fig 1a, the operator’s view was fixed to a single-point perspective, which resulted in an increase in task complexity the further away the target platform was located. The simulated environment and landing task sequence were the same for all operators.

We train neural models $\mathbf{u}_t \sim f_\theta(\mathbf{x}_t)$ to predict the operator’s action \mathbf{u}_t given the current state \mathbf{x}_t for variable tasks (i.e., different target platforms), user skill levels, and landing strategies (see Fig. 1b for examples of tele-operation trajectories with these characteristics). A tele-operation trajectory

¹Results showcasing SMCD’s performance in online, on-policy adaptation using a proportional-derivative (PD) control law for this task are shown in Appendix.

²Secondary analysis of this data was reviewed and approved by Monash University Research Ethics Committee.

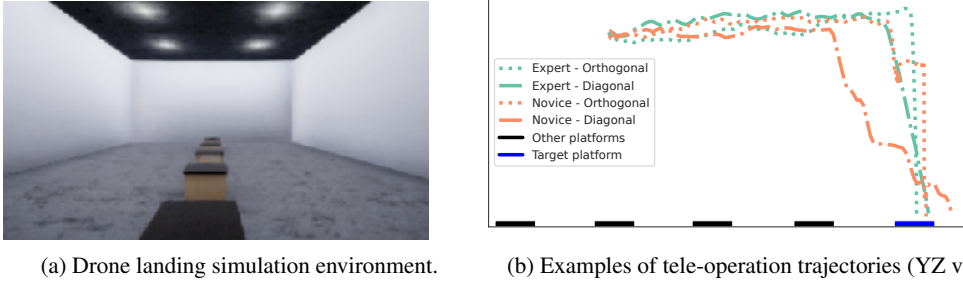


Figure 1: Drone landing data consists of tele-operation trajectories collected in a simulated environment (a). Data includes trajectories executed by operators of varying skill (one novice and one expert) and captures different landing strategies (orthogonal or diagonal) as shown in (b).

$\tau = (\mathbf{x}_1, \mathbf{u}_1, \dots, \mathbf{x}_T, \mathbf{u}_T)$ consists of a sequence of states and actions, where each state $\mathbf{x}_t = (\mathbf{p}_t, \mathbf{v}_t, d_t)$ denotes the drone’s 3D position $\mathbf{p}_t = (x_t, y_t, z_t)$, linear velocity $\mathbf{v}_t = (\dot{x}_t, \dot{y}_t, \dot{z}_t)$, and distance $d_t = \|\mathbf{g}^i - \mathbf{p}_t\|_2$ to target platform \mathbf{g}^i at time t ; and $\mathbf{u}_t = (\dot{x}_t, \dot{y}_t, \dot{z}_t)$ corresponds to the linear velocity commands provided by the human operator. We randomly split the dataset into training (83%), known-operators testing (10%), and unknown-operators testing (7%) sets.

To investigate the interpretability of the masks obtained using SMCD we evaluate whether one high-level characteristic of a trajectory (landing strategy) and one characteristic about the operator (skill level) are captured by the inferred masks³ (see Fig. 1b for trajectories showcasing these characteristics). Specifically, we measure how the prediction confidence of each target characteristic changes as the number of observed state-action pairs seen during mask inference increases. We use the distance-based confidence score proposed in [47] to evaluate this. Given the mask estimate, $\bar{\mathbf{M}}_{1:n}$, for trajectory τ obtained after n observations, with $1 \leq n < T$, let $A(\bar{\mathbf{M}}_{1:n}) = \{\bar{\mathbf{M}}_{\text{train}}^j\}_{j=1}^k$ denote the set of k -nearest masks of $\bar{\mathbf{M}}_{1:n}$ in the training set, and let $\{c^j\}_{j=1}^k$ denote the corresponding characteristic labels associated with masks in $A(\bar{\mathbf{M}}_{1:n})$. Following [47], the confidence score $D(\tau)$ for the assignment of trajectory τ to characteristic \hat{c} based on the mask estimate $\bar{\mathbf{M}}_{1:n}$ is defined as:

$$D(\tau) = \frac{\sum_{j=1, c^j=\hat{c}}^k e^{-\|\bar{\mathbf{M}}_{1:n} - \bar{\mathbf{M}}_{\text{train}}^j\|_2}}{\sum_{j=1}^k e^{-\|\bar{\mathbf{M}}_{1:n} - \bar{\mathbf{M}}_{\text{train}}^j\|_2}}. \quad (9)$$

The score $D(\tau) \in (0, 1)$ (the higher the better) is monotonically related to the local density of trajectories in the training set that share similar characteristics and lie in the neighborhood of trajectory τ , as defined by the distance between inferred masks.

5 Experimental Results

Two-link arm: look-ahead prediction results: Fig. 2 shows the root mean square prediction error (RMSE) over 1000 trials for varied burn in steps and prediction horizons (identical for all methods compared). We compare best performing models⁴ trained using multi-task pre-training (M) and Reptile meta-learning (R), and then adapted using either SMCD (S), gradient descent (G), or no adaptation (N). We also include an oracle model baseline (O) where link-length parameters in a known forward kinematics model are inferred directly using a particle filter and a latent variable model (LV) where task variability and contextual information are both captured using the low-dimensional hidden embedding, $h \in \mathcal{R}^8$, of a variational recurrent auto-encoder (VRNN) [48]. At test time, burn-in steps are used to update the VRNN’s hidden embedding later used to predict each step of the look-ahead horizon⁵.

Multi-task training with SMCD is most effective (M+S), with the exception of the oracle model. Interestingly, adaptation using gradient descent seems to exhibit more local adaptation, as prediction

³Characteristic definitions and details are provided in the [Appendix](#)

⁴Best performing models were selected following a hyperparameter search - see [Appendix](#)

⁵Since neither the multi-task nor the Reptile model networks are recurrent models, the VRNN model was constrained to train using sequences of length 2 to make the comparison between models possible.

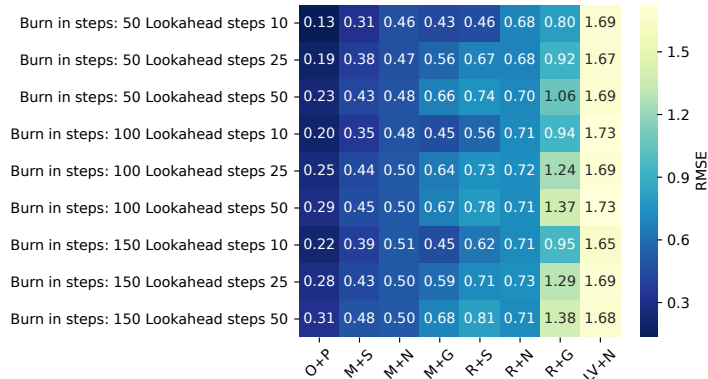


Figure 2: Look-ahead prediction errors. (O: Oracle, M: multi-task, LV: Latent Variable, R: Reptile; P: Particle Filter, S: SMCD, G: Gradient descent, N: No adaptation.)

error grows larger with look-ahead distance than when SMCD is applied. Local adaptation seems to provide an accurate model in a specific region of state space, rather than globally adapting to a particular link length. The Reptile model performs surprisingly poorly, particularly given that it was trained for substantially longer (1000 epochs) than the multi-task model (200 epochs). A similar performance is observed for the latent variable model.

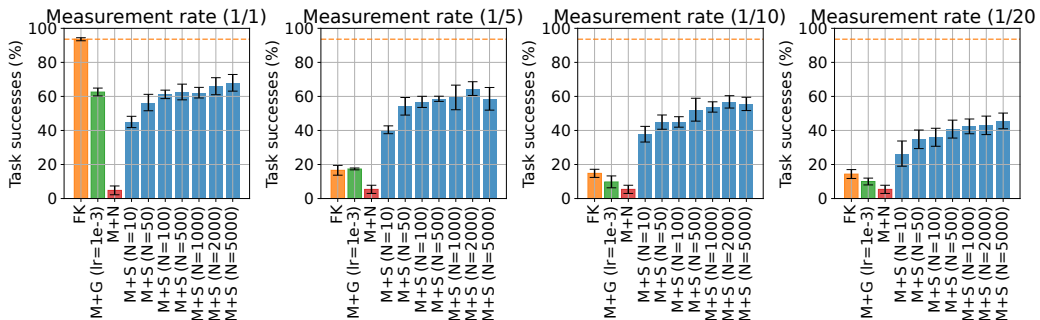


Figure 3: 7-DOF Panda manipulator control over increasing horizons. (M: multi-task, FK: Analytical, G: Gradient descent, S: SMCD, N: No adaptation) The orange line indicates best case performance when true measurements are available at every time step.

7-DOF Panda manipulator: online control results: Fig. 3 shows the success rates in the adaptive Panda control task for decreasing measurement rates. We used a 3-layer, 1024 dimensional fully connected network with ReLU activations to learn forward kinematics models. The model was trained with 100000 sampled joint angles and end-effector position combinations, with an arbitrary tool offset. A total of 100 reaching tasks were completed during testing and results averaged across 5 seeds.

We compare an analytical model (FK) that fails to account for the tool offset and a multi-task model with no adaptation (M+N), adapted using gradient descent (M+G), and adapted using SMCD (M+S). When true measurements are available at every time step, FK represents an oracle model that only fails due to singularity effects in the control law. M+G performance degrades significantly as the rate of measurement decreases and the model is required to be used for longer control periods. When selecting the M+G learning rate, we found that this performance degradation increases with learning rate, which appears to indicate that gradient descent is only suitable to adapt representations to very local contexts, and the model is no longer useful in other regions of the state space. In contrast, M+S appears to be much more effective at capturing global context, although performance still degrades when the model is used over longer periods with no feedback. Increasing the number of particles results in a moderately improved performance.

Drone landing task: mask interpretability results: Fig. 4 shows the average confidence score obtained for the prediction of the true skill level of a trajectory’s operator (i.e., novice, intermediate, or expert) and true landing strategy (i.e., orthogonal or diagonal) for all trajectories in our testing sets as the number of time steps used during mask inference increases.

Overall, we observe relatively good average confidence scores (~ 0.7) for both testing sets. This suggests that the masks inferred using SMCD contain enough global information to allow for the identification of operator skill level and the landing strategy. Both characteristics can be identified early on in the trajectory. This is particularly important for the landing strategy, which appears to change more towards the end of a trajectory. Better confidence scores are obtained for trajectories executed by unknown operators than for the known operator testing instances. This might be due to imbalances in the number of instances that belong to each possible characteristic, as visual inspection of trajectories indicated unknown operators exhibited trajectory characteristics more common in the dataset. Additional results on mask interpretability and look-ahead prediction for this task are provided in the [Appendix](#).

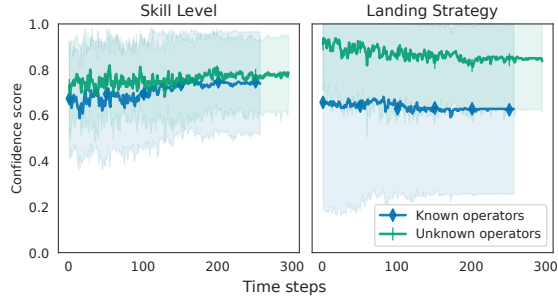


Figure 4: Average confidence score for the correct assignment of the true skill level and landing strategy for all testing trajectories (1-sigma shaded traces). Results are presented for the set of 5-nearest masks.

6 Limitations

Although neural dynamics modelling holds the potential to scale to high dimensional inputs of varied modalities, this work has mostly considered adaptation in proprioceptive state spaces. Future work should explore the potential of the proposed approach to operate in models using higher dimensional image inputs. It should be noted that control with adaptive neural models may lack the stability and safety guarantees associated with conventional dynamics modelling. Moreover, although SMCD is fast, and converges rapidly, doing so does require an energy expensive GPU. While all of the models considered in this work can be fit on a small size embedded GPU, users of the neural adaptation schemes proposed here should carefully consider their model size to determine whether sampling or back-propagation is more computationally efficient, given the relative efficacy in the multi-task training setting. Given the nature of representations learned by neural networks, this is likely to be task dependent. However, as shown above, model adaptation using SMCD can identify and adjust to contexts and unlock neural representations highly suited to model-based control in settings where gradient based adaptation schemes can result in catastrophic forgetting.

7 Conclusion

This work proposed a simple neural network adaption strategy, relying on sequential Monte Carlo adaption of the masks in a dropout regularisation network layer. These masks offer a level of interpretability, capturing both local and some global contextual information, as illustrated in a real world human behavioural modelling application. Results show that when paired with multi-task training, this simple adaptation strategy outperforms more computationally complex meta-learning schemes and overcomes some of the catastrophic forgetting problems associated with gradient descent in online adaptation settings.

Acknowledgments

We thank the reviewers for their useful comments and valuable recommendations.

References

- [1] P. A. Ioannou and J. Sun. *Robust adaptive control*, volume 1. PTR Prentice-Hall Upper Saddle River, NJ, 1996.
- [2] N. Srivastava, G. Hinton, A. Krizhevsky, et al. Dropout: a simple way to prevent neural networks from overfitting. *JMLR*, 15(1):1929–1958, 2014.
- [3] Y. Gal and Z. Ghahramani. Dropout as a Bayesian approximation: Representing model uncertainty in deep learning. In *ICML*, volume 48, pages 1050–1059, 2016.
- [4] E. D. Sontag. *Observers and Dynamic Feedback*, pages 315–345. Springer New York, New York, NY, 1998.
- [5] M. Burke. Path-following control of a velocity constrained tracked vehicle incorporating adaptive slip estimation. In *ICRA*, pages 97–102, 2012.
- [6] J. Wu, I. Yildirim, J. J. Lim, et al. Galileo: Perceiving physical object properties by integrating a physics engine with deep learning. In *NIPS*, volume 28, page 127–135, 2015.
- [7] M. Asenov, M. Burke, D. Angelov, et al. Vid2param: Modeling of dynamics parameters from video. *IEEE R-AL*, 5(2):414–421, 2019.
- [8] M. Jaques, M. Burke, and T. M. Hospedales. Physics-as-inverse-graphics: Unsupervised physical parameter estimation from video. In *ICLR*, 2020.
- [9] F. Ramos, R. Possas, and D. Fox. Bayessim: Adaptive domain randomization via probabilistic inference for robotics simulators. In *RSS*, Freiburg/Breisgau, Germany, June 2019.
- [10] L. Brunke, M. Greeff, A. W. Hall, et al. Safe learning in robotics: From learning-based control to safe reinforcement learning. *Annu. rev. control robot. auton*, 5, 2021.
- [11] C. Finn, P. Abbeel, and S. Levine. Model-agnostic meta-learning for fast adaptation of deep networks. In *ICML*, pages 1126–1135. PMLR, 2017.
- [12] A. Nichol, J. Achiam, and J. Schulman. On first-order meta-learning algorithms. *arXiv preprint arXiv:1803.02999*, 2018.
- [13] J. Snell, K. Swersky, and R. Zemel. Prototypical networks for few-shot learning. *NIPS*, 30, 2017.
- [14] F. Sung, Y. Yang, L. Zhang, et al. Learning to compare: Relation network for few-shot learning. In *CVPR*, pages 1199–1208, 2018.
- [15] S. Belkhal, R. Li, G. Kahn, et al. Model-based meta-reinforcement learning for flight with suspended payloads. *IEEE R-AL*, 6(2):1471–1478, 2021.
- [16] C. Laidlaw and A. Dragan. The boltzmann policy distribution: Accounting for systematic suboptimality in human models. *ICRL*, 2022.
- [17] S. Reed, K. Zolna, E. Parisotto, et al. A generalist agent. *arXiv preprint arXiv:2205.06175*, 2022.
- [18] A. Zhmoginov, M. Sandler, and M. Vladymyrov. Hypertransformer: Model generation for supervised and semi-supervised few-shot learning. *arXiv preprint arXiv:2201.04182*, 2022.
- [19] A. Gupta, L. Fan, S. Ganguli, and L. Fei-Fei. Metamorph: Learning universal controllers with transformers. *arXiv preprint arXiv:2203.11931*, 2022.
- [20] J. Kirkpatrick, R. Pascanu, N. Rabinowitz, et al. Overcoming catastrophic forgetting in neural networks. *Proceedings of the national academy of sciences*, 114(13):3521–3526, 2017.

- [21] E. Grant, C. Finn, S. Levine, et al. Recasting gradient-based meta-learning as hierarchical Bayes. *arXiv preprint arXiv:1801.08930*, 2018.
- [22] J. Yoon, T. Kim, O. Dia, et al. Bayesian model-agnostic meta-learning. *NIPS*, 31, 2018.
- [23] O. Miglino, H. H. Lund, and S. Nolfi. Evolving mobile robots in simulated and real environments. *Artificial life*, 2(4):417–434, 1995.
- [24] K. O. Stanley and R. Miikkulainen. Evolving Neural Networks through Augmenting Topologies. *Evolutionary Computation*, 10(2):99–127, 06 2002.
- [25] J. Schmidhuber, D. Wierstra, M. Gagliolo, and F. Gomez. Training Recurrent Networks by Evolino. *Neural Computation*, 19(3):757–779, 03 2007.
- [26] T. Salimans, J. Ho, X. Chen, et al. Evolution strategies as a scalable alternative to reinforcement learning. *arXiv preprint arXiv:1703.03864*, 2017.
- [27] P.-T. De Boer, D. P. Kroese, S. Mannor, and R. Y. Rubinstein. A tutorial on the cross-entropy method. *Annals of operations research*, 134(1):19–67, 2005.
- [28] M. Kobilarov. Cross-entropy motion planning. *IJRR*, 31(7):855–871, 2012.
- [29] S. Imai, S. Kawai, and H. Nobuhara. Stepwise pathnet: a layer-by-layer knowledge-selection-based transfer learning algorithm. *Scientific Reports*, 10(1):1–14, 2020.
- [30] S. Anwar, K. Hwang, and W. Sung. Structured pruning of deep convolutional neural networks. *ACM Journal on Emerging Technologies in Computing Systems (JETC)*, 13(3):1–18, 2017.
- [31] C. L. Baker, R. Saxe, and J. B. Tenenbaum. Action understanding as inverse planning. *Cognition*, 113(3):329–349, 2009.
- [32] M. Chen, S. Nikolaidis, H. Soh, et al. Trust-aware decision making for human-robot collaboration: Model learning and planning. *ACM THRI*, 9(2):1–23, 2020.
- [33] P. Carreno-Medrano, S. L. Smith, and D. Kulix0107;. Joint estimation of expertise and reward preferences from human demonstrations. *IEEE TRO*, pages 1–18, 2022.
- [34] L. Peternel, N. Tsagarakis, D. Caldwell, and A. Ajoudani. Adaptation of robot physical behaviour to human fatigue in human-robot co-manipulation. In *Humanoids*, pages 489–494. IEEE, 2016.
- [35] S. Nikolaidis, D. Hsu, and S. Srinivasa. Human-robot mutual adaptation in collaborative tasks: Models and experiments. *IJRR*, 36(5-7):618–634, 2017.
- [36] D. Fridovich-Keil, A. Bajcsy, J. F. Fisac, et al. Confidence-aware motion prediction for real-time collision avoidance. *IJRR*, 39(2-3):250–265, 2020.
- [37] D. Vogt, S. Stepputtis, S. Grehl, et al. A system for learning continuous human-robot interactions from human-human demonstrations. In *ICRA*, pages 2882–2889, 2017.
- [38] B. Wang, E. Adeli, H.-k. Chiu, et al. Imitation learning for human pose prediction. In *ICCV*, pages 7124–7133, 2019.
- [39] M. Carroll, R. Shah, M. K. Ho, et al. On the utility of learning about humans for human-AI coordination. *Advances in neural information processing systems*, 32, 2019.
- [40] C. Rudin. Stop explaining black box machine learning models for high stakes decisions and use interpretable models instead. *Nature Machine Intelligence*, 1(5):206–215, 2019.
- [41] A. Doucet, S. Godsill, and C. Andrieu. On sequential Monte Carlo sampling methods for Bayesian filtering. *Statistics and computing*, 10(3):197–208, 2000.
- [42] D. Crisan and A. Doucet. A survey of convergence results on particle filtering methods for practitioners. *IEEE TSP*, 50(3):736–746, 2002. doi:10.1109/78.984773.

- [43] A. Kong, J. S. Liu, and W. H. Wong. Sequential imputations and bayesian missing data problems. *JASA*, 89(425):278–288, 1994.
- [44] R. M. French. Catastrophic forgetting in connectionist networks. *Trends in cognitive sciences*, 3(4):128–135, 1999.
- [45] P. Corke and J. Haviland. Not your grandmother’s toolbox—the robotics toolbox reinvented for python. In *2021 IEEE International Conference on Robotics and Automation (ICRA)*, pages 11357–11363. IEEE, 2021.
- [46] K. Backman, D. Kulić, and H. Chung. Learning to assist drone landings. *IEEE R-AL*, 6(2): 3192–3199, 2021.
- [47] A. Mandelbaum and D. Weinshall. Distance-based confidence score for neural network classifiers. *arXiv preprint arXiv:1709.09844*, 2017.
- [48] O. Fabius, J. R. van Amersfoort, and D. P. Kingma. Variational recurrent auto-encoders. In *ICLR (Workshop)*, 2015.
- [49] S. Sæmundsson, K. Hofmann, and M. P. Deisenroth. Meta reinforcement learning with latent variable gaussian processes. *arXiv preprint arXiv:1803.07551*, 2018.
- [50] Z. Mandi, P. Abbeel, and S. James. On the effectiveness of fine-tuning versus meta-reinforcement learning. *arXiv preprint arXiv:2206.03271*, 2022.
- [51] I. Clavera, A. Nagabandi, S. Liu, et al. Learning to adapt in dynamic, real-world environments through meta-reinforcement learning. In *ICLR*, 2019.
- [52] G. Williams, A. Aldrich, and E. A. Theodorou. Model predictive path integral control: From theory to parallel computation. *Journal of Guidance, Control, and Dynamics*, 40(2):344–357, 2017.
- [53] A. Nagabandi, G. Kahn, R. S. Fearing, and S. Levine. Neural network dynamics for model-based deep reinforcement learning with model-free fine-tuning. In *ICRA*, page 7559–7566, 2018.

This appendix is structured as follows: we introduce multi-task model and SMCD ablations results, a detailed description of baseline models, and additional prediction and mask interpretability results for the two-link arm task in Appendix A. We describe data labelling, multi-task model ablations and additional results on mask interpretability and look-ahead prediction for the drone-landing task in Appendix B. In Appendix C, we show how multi-task model training and SMCD adaptation can be used in a model-based Reinforcement Learning setting. Finally, we describe additional properties of the proposed SMCD method in Appendix D.

A Two Link-Arm - Forward Kinematics Task

A.1 Multi-Task Model Ablations

We completed a hyper-parameter sweep of latent dimension, dropout probability, learning rate, batch size, and the number of epochs to find the best multi-task pre-training model for evaluation in prediction and control. Fig. 5 shows the training loss (mean square prediction error) for all hyper-parameters. Results indicate that the best training loss is achieved by models of medium-to-large size (latent dimensions 512 and 1024), with a dropout probability of $p = 0.5$, and learning rate of $1e^{-4}$. Furthermore, we observe the batch size has little to no effect, and models converge quickly after approximately 100 epochs.

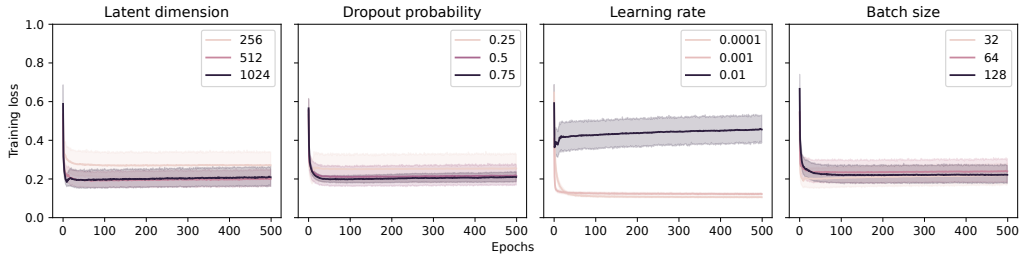


Figure 5: Training loss for all possible hyper-parameters. Each plot shows how the training loss changes when one parameter is fixed (e.g., latent dimension) and the remaining ones take on all possible values.

The same space of parameters was used to find the best Reptile model. Two additional hyper-parameters, the inner learning rate (set to 0.02) and the inner number of epochs (set to 1), were kept constant during the search.

A.2 SMCD Prediction Ablations

A hyper-parameter sweep (bit flip transition probability, measurement noise σ_r , dropout probability, number of particles, and latent dimension) showed that prediction error when using SMCD adaptation is primarily affected by the dropout probability used at training ($p=0.5$ appeared most effective), followed by the dimensionality of the network layers, indicating that model capacity is important to capture the prediction uncertainty arising from the link length variability. Fig. 6 shows the mean square prediction error for a range of look ahead horizons after a certain number of burn-in adaptation steps sorted by hyper-parameter. It is clear that latent dimension (model capacity) plays the biggest role in adaptation efficacy, and that the filter is relatively robust to changes in transition probability, likelihood noise and mask particle numbers.

A.3 Adaptation Baselines

For the 2-Link forward kinematics prediction task we compared against a Reptile model. The base network (3-layer NN, with ReLU activations) is identical to the model trained using multi-task training and trained on the same dataset. However, instead of sampling data at random, training is sampled by task. We conducted a similar hyper-parameter sweep as in Fig. 5 and selected the best performing model for comparison. We briefly discuss the baselines and draw attention to some noteworthy aspects of their performance below.

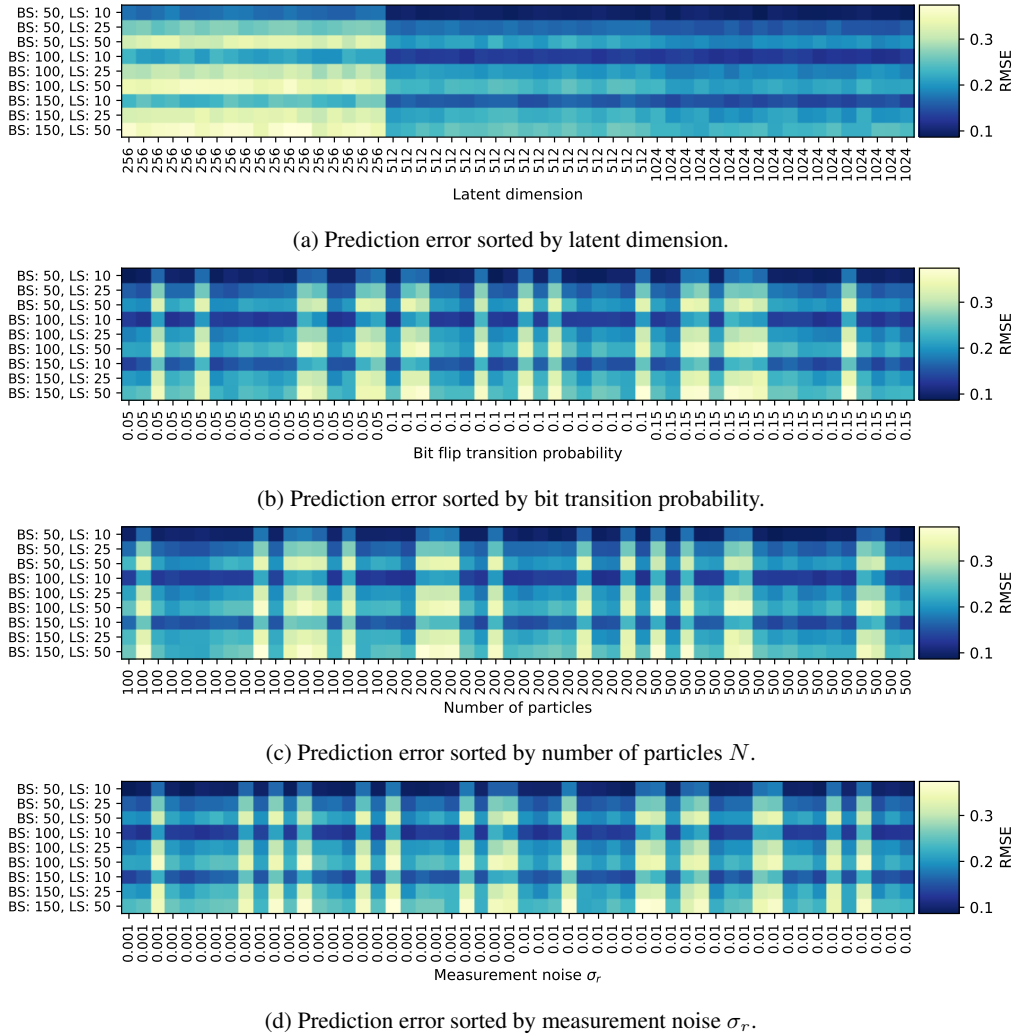


Figure 6: SMCD look-ahead mean squared prediction error for various mask dimensions sorted all parameters considered during hyper-parameter sweep (BS: Burn in adaptation steps, LS: Look-ahead prediction steps.)

- **R+S:** By training the model using Reptile and dropout regularisation, we can apply SMCD for online adaptation. Results show this is relatively effective, and that SMCD can be used alongside meta-learning approaches. We also observe that adapting a model trained using multi-task training appears to be more effective.
- **R+N:** As a meta-learning approach, Reptile seeks to find a representation that can rapidly be adapted to produce low prediction error in new settings with relatively few gradient steps. This means the initial representation may not result in low prediction error. In contrast, the multi-task training approach performs empirical risk minimisation, that is, it seeks to find a model with low prediction error across all settings or task variations. As a result when no adaptation is applied, we find that multi-task training (M+N) is generally more effective.
- **R+G:** Our results show that Reptile performs poorly in a look-ahead prediction setting compared to our proposed approach. A similar trend was observed in an online setting (i.e., adaptation control experiment). Typically, meta-learning strategies like Reptile are adapted to new tasks by collecting and storing large buffers of task specific observations, and then performing a *global* model update using a number of stochastic gradient descent iterations.

In a rapidly changing online setting, this is infeasible, and produces additional challenges. Specifically, we can choose to update with a higher learning rate and risk destroying the underlying representation by over-fitting to a local context (this is what appears to happen in R+G), or update very slowly so as to not stray too far from the initial representation (something closer to R+N) resulting in extremely slow convergence. A core benefit of SMCD is that it provides an explicit online update rule, which alleviates these problems.

- **LV+N**: The proposed SMCD method captures task variability and contextual information through a combination of all the weights of the multi-task learned neural model and the inferred dropout masks. Other approaches in the literature do so by explicitly learning a low-dimensional latent embedding (e.g., [49]). To test whether the proposed approach leads to better performance at the cost of a higher-dimensional embedding, we compared against a recurrent variational auto-encoder with a hidden embedding of dimensionality 8. The VRNN model was trained on the same data set as the multi-task model for a total of 200 epochs. Our results indicate that this latent model performs poorly compared to the proposed SMCD model. This can be partially due to the length of the sequences chosen to train the model. Since the multi-task model has no recurrent layer, we limited the sequences fed to the VRNN during training to a length of two time-steps in order to make both models comparable. It is possible that the VRNN model achieves better performance if trained over longer sequences.

The relative performance difference between simple multi-task learning and Reptile observed in our experiments agrees with a recently released work directly comparing multi-task training and fine tuning with meta-learning in RL settings, which corroborates our findings [50]. This large scale study across a broad benchmark of meta-RL tasks concludes that multi-task training performs equally as well or better than meta-RL on similar levels of data.

A.4 Online Adaptation during Control

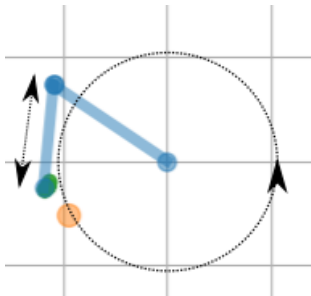


Figure 7: A 2-link arm with sinusoidally varying length l_2 following a moving target.

We also evaluated the performance of SMCD in control (see Fig. 7) using the two-link arm task. Here, we control the two-link manipulator to follow a moving target \mathbf{x}_g around a circle of radius $r \sim U(0.3, 1.5)$, with starting angle $\phi \sim U(-\pi, \pi)$, measured relative to the base of a randomly initialised manipulator. We use the PD control law $\mathbf{u} = -K_1 \mathbf{J}^\dagger (\mathbf{x} - \mathbf{x}_g) - K_2 \dot{\mathbf{q}}$ to follow the moving target ($K_1 = 20, K_2 = 5$). Here, \mathbf{J}^\dagger is the Moore-Penrose pseudo-inverse of the Jacobian of the network $f_\theta(\mathbf{q})$. In order to test online forward kinematics adaptation, we consider a telescoping second link, with sinusoidally varying length $l_2 = 1 + 0.25 \sin(\pi k/20)$, with timestep $k \in (0, 100)$. This experiment evaluates convergence speed in response to an initial disturbance, alongside continual online adaptation ability. We benchmark against an oracle model, no adaptation and a model trained using Reptile [12], a first order meta-learning approach, and investigate adaptation using both gradient descent and SMCD.

Fig. 8 shows the average control error for the online control task with sinusoidally varying links, across 1000 repetitions. Results are shown for the best performing reptile and multi-task trained models for no adaptation (None), online gradient descent adaptation (GD) and online sampling-based adaptation (SMCD). As in the look-ahead prediction case, multi-task training with SMCD adaptation is most effective, producing rapid convergence to the moving goal when used for control. Interestingly, particle filtering with a known model (Oracle+PF) struggles to deal with the rapidly changing forward kinematics, but adaptation in mask space or by gradient descent converges much faster.

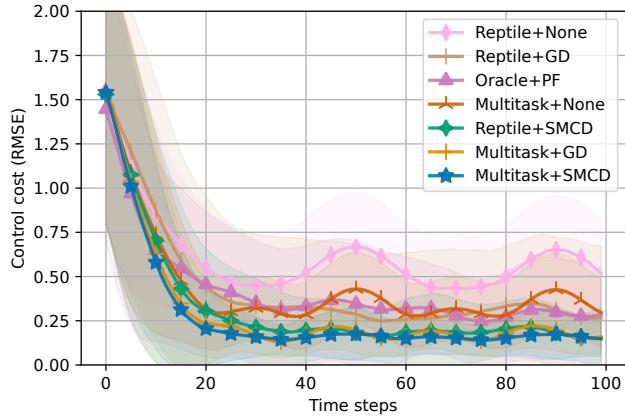


Figure 8: Closed-loop PD control of a 2-link arm following a moving target with a sinusoidally telescoping link (1-sigma shaded traces).

A.5 Mask Interpretability

To investigate whether the inferred masks capture information about link lengths, we evaluated top k classification accuracy using the masks, where accuracy is determined by calculating the frequency with which the nearest neighbour in link space (euclidean distance between link lengths) lies within the top k nearest neighbours in mask space (euclidean distance between masks). Fig. 9 shows that the masks do contain information about link lengths, and that the capacity to do so increases with model latent dimensionality ld . Inspection of the distances between masks show that there can be many masks corresponding to a good prediction in a particular angle or link-length configuration. This allows for rapid adaptation, as the mask inference mask space does not need to converge to only one of the 2^d possible masks.

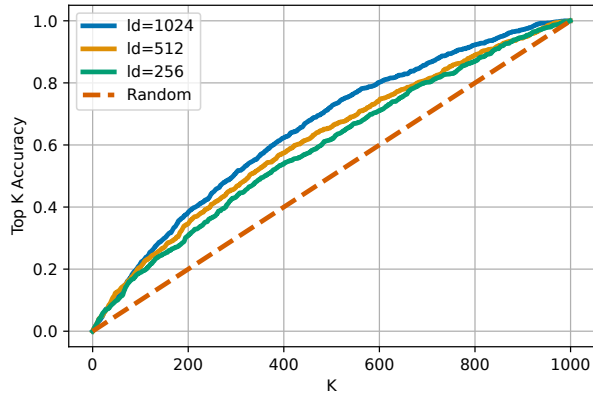


Figure 9: Evaluating link length information captured by inferred masks.

B Drone Landing Task

B.1 Human Data Labelling

A total of four high-level characteristics were tested when evaluating mask interpretability for the drone landing example. These characteristics are landing strategy, operator’s skill level, flight phase, and the likelihood of success.

The landing strategy of each trajectory in the dataset was manually assigned after visually inspecting each trajectory. For the flight phase, it was assumed that a tele-operation trajectory is composed of two phases: approach (the drone moves forward toward the target platform) and descent (the drone comes down to the target platform). An example is shown in Fig. 11. The start and end of each phase were manually defined after visually inspecting each trajectory.

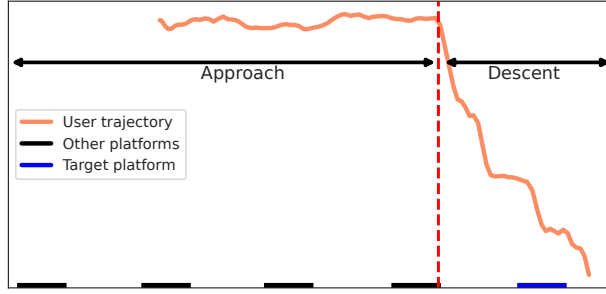


Figure 10: Segmentation of a tele-operation trajectory into two stages: approach (the drone moves forward toward the target platform) and descent (the drone comes down to the target platform).

A trajectory was labelled as successful if and only if the drone’s height at the end of the trajectory was inferior to the height of the target platform height and the drone’s final position in the XY plane laid within the boundaries platform’s top face. To determine an operator’s skill level, we computed the number of successful landings for each operator and analysed the operators’ performance distribution. We found that performance was normally distributed (see Fig. 11) and proceeded to split users into one of three groups: novices (10% low performers), experts (10% top performers), and intermediate (average performers).

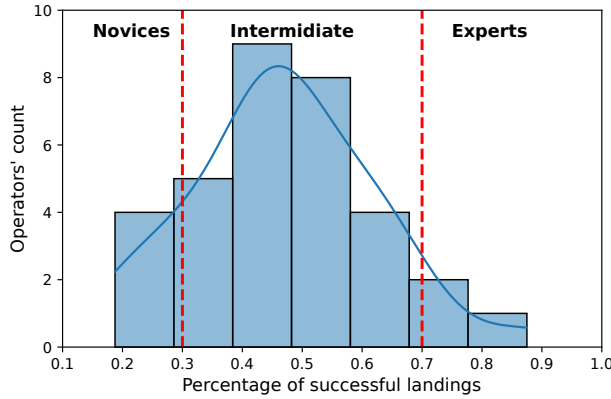


Figure 11: Distribution of operator’s performance. Operators in the top and bottom 10% were labelled experts and novices, respectively.

B.2 Multi-Task Model Ablations

A hyper-parameter sweep (latent dimension, dropout probability, learning rate, batch size, and the number of epochs) was done to find the best multi-task pre-training model for the drone landing task. Only a subset of the training dataset was used in the search (192 trajectories). We limited the number of epochs to 100 based on the fast convergence observed for the forward kinematics example. Fig. 12 shows the training loss (mean square prediction error) for all hyper-parameters. Results seem to indicate that models of medium-to-large size (latent dimensions 512 and 1024), with a dropout probability of $p = 0.5$, learning rates of $1e^{-4}$, and batch size of 64 samples performed the best during training.

The Reptile model used in the evaluation look-ahead prediction error was set to have the same hyper-parameters as the best multi-task pre-training model found during the search. The two additional hyper-parameters required by the reptile model (the inner learning rate and the inner number of epochs) were fixed to the same values used for the forward kinematics tasks.

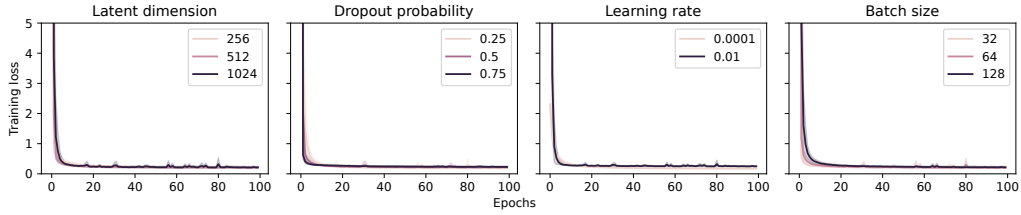


Figure 12: Training loss for all possible hyper-parameters. Each plot shows how the training loss changes when one parameter is fixed (e.g., latent dimension) and the remaining ones take on all possible values.

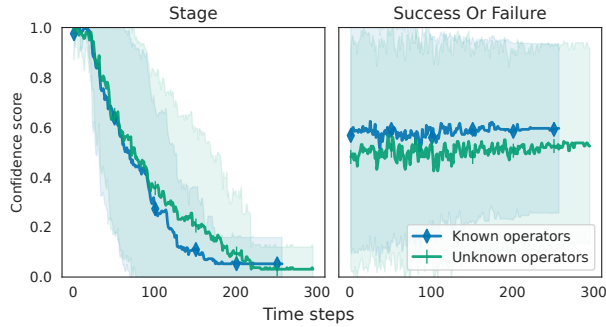


Figure 13: Average confidence score for the correct assignment a trajectory's stage and likelihood of success for all testing trajectories (1-sigma shaded traces). Results are presented for the set of 5-nearest masks.

B.3 Mask Interpretability - Additional Results

Fig. 13 shows the average confidence scores obtained for the current stage of a given trajectory (approach or descent) and whether this trajectory will end in a successful or failed landing. Results are shown for all trajectories in our testing sets.

Overall, although we can identify with high confidence (approx. 1.0) the approach stage of a trajectory (left plot), the masks inferred later on fail to encode enough information to allow for the correct identification of the descent stage. Similarly, the confidence scores for the prediction of success or failure are slightly above the chance level (~ 0.55) for the trajectories of both known and unknown operators. These results indicate that although the inferred masks capture some contextual information about trajectories and operators, not all of the high-level characteristics we have identified as important can be predicted through a simple mask comparison process.

B.4 Look-Ahead Prediction Error

We further assessed the performance of the proposed approach in look-ahead prediction using the drone landing task. Specifically, we evaluated prediction error on trajectories obtained from known (some trajectories were seen during training) and unknown (all trajectories excluded during training) operators.

Fig. 14 shows the RMSE for held-out tele-operation trajectories. We consider two test sets: known (left) and unknown (right) operators for varied burn in and prediction horizon ratios. We use ratios instead of steps since trajectories are of varying lengths. As with the two-link example, we compare the best performing models trained using multi-task pre-training and Reptile meta-learning, with and without adaptation. Note that multi-task pre-training without adaptation corresponds to a behaviour cloning approach to action prediction.

As expected, the look-ahead prediction error obtained for trajectories executed by known operators is lower than the error rates obtained for the unknown operator trajectories. However, as initially observed in the two-link arm example, this difference in performance grows smaller as the duration

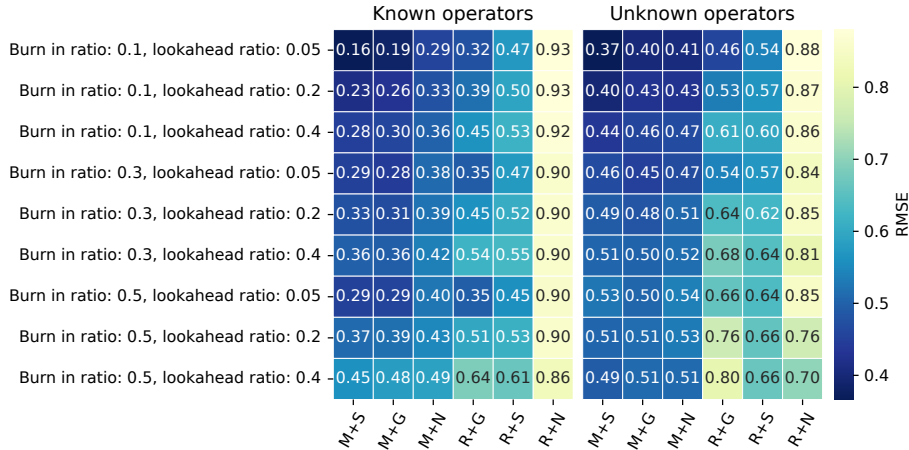


Figure 14: Look-ahead prediction errors for human data, ordered by performance. (M: multi-task, R: Reptile, G: Gradient descent, S: SMCD, N: No adaptation).

of the adaptation and look-ahead prediction horizons increases. This suggests that rather than globally adapting to a particular task instance or operator’s tele-operation style, the proposed approach is better at providing accurate models in specific regions of the state space. In terms of overall model performance, we observe that multi-task training with SMCD is most effective, followed by multi-task training with Gradient Descent adaptation. Once again, the model trained using Reptile performs poorly even when trained for substantially longer (1000 epochs) than the other models (400 epochs).

C SMCD Application to Reinforcement Learning Settings

C.1 Quadrupedal Robot (Ant)

We also consider a continuous control task from the OpenAI Gym suite. In this task, the goal is to make a four-legged robot to move forward as quickly as possible. We employ the task implementation first introduced in [51] in which the robot’s observed state o_t ⁶ and action u_t spaces are high-dimensional, i.e., $o_t \in \mathcal{R}^{41}$ and $u_t \in \mathcal{R}^8$. We use multi-task training with dropout to approximate the robot dynamics and compare different combinations of model-based controllers (Cross Entropy Method - CEM [28], Model Predictive Path Integral - MPPI [52], and Random Shooting - RS [53]) and adaptation strategies (No adaptation, SMCD, and gradient descent) during an online control task. During evaluation, we randomly sample a leg to cripple on this quadrupedal robot. This task measures the ability of the proposed approach to work in high-dimensional spaces and adapt to an unexpected and drastic change to the underlying dynamics. We note that the approximate dynamic model is trained using samples in which all legs are functional.

C.2 Online Control Results

Fig. 15 shows the average reward obtained for a range of model-based RL control strategies, along with gradient and SMCD model adaptation. We used a 3-layer, 1024 dimensional fully connected network with ReLU activations to learn the approximate dynamics model of the quadrupedal robot. The model was trained with 1000000 randomly sampled state-action pairs obtained in an environment where all legs could be actuated. The average rewards reported in Fig. 15 were obtained after completing 110 episode rollouts of 1000 steps each for both the normal and randomly crippled-leg environment. The same setup was applied for each controller and adaptation strategy combination.

Both adaptation strategies perform similarly here, in and out of distribution. Importantly model adaptation does improve control performance, particularly when drastic changes in the underlying dynamics are introduced (right-plot). These results suggest that the proposed approach is also

⁶This observation representation includes the torso position and orientation, joint angles, the torso linear and angular velocity, joint velocities, and the Cartesian orientation and centre of mass.

suitable for high-dimensional task spaces. However, it should be noted that there is significant confounding arising from the controller performance (no model-specific parameter tuning was performed for each controller) and the sampling strategy used to gather training data (all samples were obtained using randomly chosen actions), which may not adequately reflect the performance of the underlying adaptation strategies across all regions of the state space to the extent that the Panda control experiments test. It is likely that improved RL control and exploration strategies are needed to fully reap the benefits of SMCD.

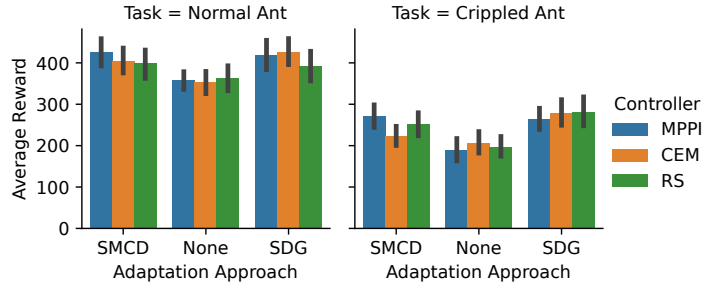


Figure 15: Average reward obtained for the quadrupedal robot online control task. Results are shown for rollouts sampled from both inside (i.e., all legs are functional (left plot)) and outside (i.e., one leg is randomly crippled (right plot)) of the training distribution.

D Additional Properties of SMCD

D.1 Minimum Mean Square Estimator

For control oriented tasks we use a minimum mean square estimator (MMSE) to find a single mask for prediction. This is a good choice of estimator if the distribution over masks is uni-modal. Our primary motivation for choosing this estimator was speed - a MAP estimator would require some level of density estimation and maximisation. Our control experiments did not show problems with estimates arising from multi-modality, and the update rule considers the full distribution. This suggests that the MMSE is not vulnerable to issues arising from this. We suspect that severe multi-modality will result in an average mask with values close to 0.5, which in turn results in a prediction close to the empirical risk minimising mean we’d receive after multi-task training with dropout.

D.2 Computational Complexity

SMCD relies on N forward passes through the network, where N is the number of masks. Although these can be easily batched, this does have an increased memory footprint when compared to gradient based approaches, which require approximately twice the number of model parameters. This greater memory footprint allows for a faster update scheme and more rapid adaptation.

Importantly, SMCD relies on a standard bootstrap particle filter, which breaks the curse of dimensionality – convergence is independent of the state dimension (mask size) and the rate of convergence is in $\frac{1}{N}$ [42]. There is extensive theory on choosing N for filters of this form [43], and the formulation allows for variable batch sizes if desired, to allow even more efficient adaptation.

As a result, we believe the proposed approach is highly scalable, particularly given the typical VRAM associated with modern GPUs, where batch sizes of 100 (see ablations above for particles) are entirely feasible for models of the size typically used in robot control⁷.

⁷Our largest model with 5000 particles used 3GB of GPU VRAM